RASĀYAN *J. Chem.*
Vol. 16 | No. 1 |456-462| January - March | 2023
ISSN: 0974-1496 | e-ISSN: 0976-0083 | CODEN: RJCABP
http://www.rasayanjournal.com
http://www.rasayanjournal.co.in

In-situ HYDROTHERMAL METHOD FOR GRAPHENE OXIDE/HYDROXYAPATITE SYNTHESIS FROM SCALLOP SHELLS

D. M. Islami[1], Wulandari[1], N. Jamarun[1,✉], Syukri[1] and V. Sisca[2]

[1]Department of Chemistry, Faculty of Mathematics and Natural Sciences, Universitas Andalas, Padang, Indonesia, 25163.

[2]Department of Biology Education, STKIP YPM Bangko, Jambi, Indonesia, 37313.

✉ Corresponding Author: novesarjamarun@sci.unand.ac.id

ABSTRACT

The graphene oxide/hydroxyapatite composite was synthesized using an in situ hydrothermal method. In this process, scallop shells (Amusium pleuronectes) were used as a source of calcium ions in fabricating the composite. Meanwhile, graphene oxide was exfoliated and oxidized from graphite powder. X-ray diffraction confirms that hydroxyapatite in the composite has a hexagonal structure. Also, the inclusion of graphene into the system did not alter the crystal structure. However, it affected the size of the apatite crystal deposited in the graphene surfaces layer, which was revealed by scanning electron microscopy analysis. The infrared spectra confirm some shiftings of the phosphate bands absorption, indicating electronic interaction between graphene and apatite matrix. Furthermore, from the Electron dispersive X-ray analysis obtained ratio of calcium/phosphate was found to be 1.84.

Keywords: *Amusium Pleuronectes*, Hydroxyapatite, Graphene Oxide, Composite, In-Situ Hydrothermal, Seashells.

RASĀYAN *J. Chem.*, Vol. 16, No.1, 2023

INTRODUCTION

Hydroxyapatite (HAp) is one of many forms of calcium phosphates ceramic with $Ca_{10}(PO_4)_6(OH)_2$ as its structural formula.[1] It has good biocompatibility, bioactivity, and osteoconductivity behaviors. It is chemically akin to bone matrix composition and thermodynamically stable in body fluid systems. These features led HAp to be further used in many areas of the biomedical field, especially in orthopedics and orthodontics for implants and coating or load bone-bearing repair materials.[2–4] However, HAp has some drawbacks that limit its total performance. Some are brittle, weak in toughness and hardness, and low in elastic modulus.[5–7] Thus, to increase the ability of HAp for biomedical purposes, combining HAp with other materials as reinforced could be a solution. Several other materials have been used to produce a hybrid compound with HAp. Those were metals, oxides, polymers, and carbon-based materials.[8] Many carbon compounds were used as reinforced materials for HAp.[9] One of them is graphene, especially in its functional form, graphene oxide (GO). GO is a unique 2D planar carbonaceous compound that is formed by introducing groups containing oxygen such as hydroxyl, epoxides, carboxyl, and carbonyl groups covering the basal surface area of GO through the reaction of oxidation.[10] These functional groups cause GO become soluble in water. Nonetheless, it has appropriate biocompatibility and osteoconductivity. A report advises that it can accommodate the cell's adhesion and proliferation, which drove its attention to be applied in biomedical fields.[11,12] In addition to that, the establishment of HAp with GO enhances the weak virtue of HAp because the strength of GO favors the weak properties of HAp, allowing its utilization in many areas, including as reinforced for implants or coating materials, especially for load bone-bearing repair applications.[13] Also, compared to pure HAp, composite GO/HAp shows better performance in those areas. Several approaches and methods have been used in generating GO/HAp composite, such as precipitation[14], hydrothermal[15], sol-gel[16], and electro-deposition.[8] In this work, we used an in situ hydrothermal method to create GO/HAp composite. Another outcome is an approach to changing the precursor for GO/HAp synthesis. Instead of synthetic calcium source compounds, we used natural waste materials to provide ion Ca^{2+} in making GO/HAp synthesis. These materials are calcium abundance materials. Some reports have used animal bones, egg shells, coral reefs, and sea shells as a source of calcium to produce Hap.[17,18,19]

http://doi.org/10.31788/RJC.2023.1618169
This work is licensed under a CC BY 4.0 license.

However, the employment of waste calcium-based material in GO/HAp composite preparation, primarily through in situ hydrothermal, still needs to be made available. Therefore, this work aimed to produce the composite by using scallop shells *"Amusium pleuronectes,"* collected in the local food industry as calcium precursors through in situ hydrothermal method. Nonetheless, this approach can also solve environmental issues created by industrial food waste and will increase the value of the waste sea shells.

EXPERIMENTAL

Material and Methods

The precursors of synthesis (Graphite, $KMnO_4$, H_2SO_4, H_2O_2, HCl, NH_4OH, $(NH_4)_2HPO_4$, and HNO_3) were collected commercially and pure analytical grades. The reagents were used without further purification. Bidistilled water was applied in all experiments. The waste scallop shells, as a resource of Ca^{2+} ions, were collected from a local seafood restaurant.

Preparation of HAp From Scallop Shells

The scallop shells were washed and dried to obtain the powder and used to produce PCC through the carbonation method. Then, obtained PCC was used as the Ca^{2+} ion source to synthesize HAp by diluting it with 20 mL HNO_3 into a calcium nitrate solution. 0,5 M (20 mL) $(NH_4)_2HPO_4$) solution was gradually dropped, and the mixture's pH was controlled to 10 by adding ammonia while stirring. After 30 minutes, hydroxyapatite was transferred into an autoclave and underwent the hydrothermal process at 180 ^oC for 6 h. Finally, HAp particles were rinsed with bidistilled water and dried overnight.

Preparation of GO/HAp Composites

The graphene oxide was prepared according to the modified Hummers method. Next, GO was sonicated for 40 minutes in bidistilled water. Into the dispersion, $Ca(NO_3)$ solution was dropwise added and stirred for 1 h. Phosphate solution was added after 1 h reaction occurred, then ammonia was incorporated into the mixture until pH reached 10 and stirred for the next 30 minutes. The suspension was moved into an autoclave the hydrothermal process was kept for 6 h at 180 ^oC. Following that, the suspended powder was rinsed and dried overnight at 60 ^oC. In this work, GO concentration was varied 1,5 wt%, 2,0 wt% and 2,5 wt% and labeled as GO-1/HAp, GO-2/HAp and GO-3/HAp respectively.

Characterization

The scallop shell composition was analyzed using XRF (PANalytical). Afterward, the crystallinity of each sample was determined using XRD (XPERT PRO PANalytical). The interactions of the chemical bonds on the samples were investigated using FT-IR (Perkin Elmer). The surface morphology was observed using SEM (Hitachi Flexsem).

RESULTS AND DISCUSSION

Preliminary Analysis of Scallop Shell

The scallop shell was used as a calcium source to synthesize the composites. Before being used, the shells were analyzed with XRF to determine the compositions. As explained in Table-1 suggested that around 96% of the shells were dominated by calcium. In order to obtain the high purity of hydroxyapatite, The shells were processed to be precipitated calcium carbonate (PCC) through the carbonation method. The structural analysis of obtained PCC was carried out using X-ray diffraction. From Figure-1, it can be seen that PCC consisted of all peaks that are characteristic of calcium carbonates compared to the ICSD standards. The XRD pattern confirms two types of carbonate crystals: calcite (ICSD #172232) and vaterite (ICSD #27827).[20,21] The polymorph formation was affected by the pH and temperature reaction.[22]

X-ray Diffraction Analysis

Figure-2 shows the diffraction pattern of GO, GO/HAp composites, and HAp. The diffraction pattern of GO exhibits a sharp peak around $2\theta = 10^o$. It clarifies that graphite was successfully oxidized using a modification of Hummer's method, which resulted in GO. From that, we also can understand that the intense peak cites as the oxidation of graphite promoted the introduction of new surface groups such as epoxides, carboxylic, and hydroxyl, causing the d-spacing between layers of GO increased to 0.90 nm. On the other hand, similar characteristics of all peaks were indexed as 25.9 (002), 31.7 (211), 32.2 (112), 32.9 (300), 34.0 (202), 39.7 (130), 46.6 (222), 49.5 (213), and 53.2 (004) correspond to both GO/HAp

composites and HAp which exactly matched with standard ICSD #16742.[23–25] According to Fig.-2, the peaks of each obtained sample were in good crystallinity and depicted a hexagonal crystal system with space group P63/M and lattice constant value a = b = 9.4320 and c = 6.8810.

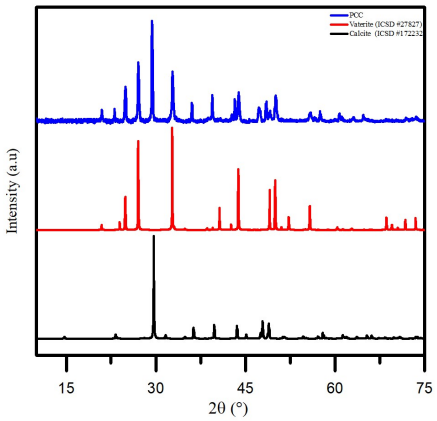

Fig.-1: XRD Patterns of Precipitated Calcium Carbonate (PCC)

Table-1: The Composition Analysis of Scallop Shells

Scallop shells composition (%)	
CaO	96.443
Ag_2O	0.579
SrO	0.289
Al_2O_3	0.463
SiO_2	0.293
Others	1,933

Then, it can be concluded that GO inside the HAp matrix did not change its lattice parameter, but it influenced the crystal size of HAp in the composite system, as mentioned in Table-2. However, during the hydrothermal process at 180 °C, GO changed into r-GO.[26] This reduction process was physically proven by the color change of the composite after hydrothermal from milky brown suspension into grayish-colored powder. Then, it was also confirmed by the diffraction peak at 2θ = 26°. However, this peak overlapped with a peak at (002) of HAp. Although the overlapping occurred, the transition GO to r-GO in composite formation was still indicated by the decreasing of the peak intensity of HAp.[27]

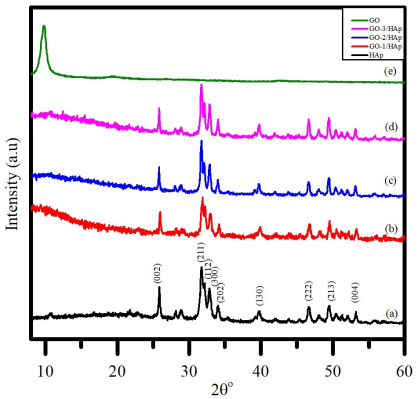

Fig.-2: Diffraction Pattern of GO, GO/HAp, and HAp

Fourier Transform Infrared Analysis

Figure-3 provides each spectrum of GO, GO/HAp composites, and HAp. It shows that the bending vibration (v2) of the PO_4^{3-} bond was assigned at 473 cm^{-1}. Next, the regions of bands from 563 – 603 cm^{-1} were denoted as bending vibration (v4) of the PO_4^{3-} bond. At the same time, the bending vibration (v3) and stretching (v1) of PO_4^{3-} bonds were defined at 1041 and 1091 cm^{-1}, respectively.[28-30] Subsequently, the stretching of the OH bond of HAp structure and absorbed water were recorded at 633 cm^{-1} and 3436 – 3572

cm^{-1}. The exact peaks happened for GO/HAp composites. This is caused by the small concentration of GO used in composites and the bands that correspond to it overlapped with HAp spectra and as proof that the addition of GO does not alter the chemical structure of HAp.[15] The interaction between GO and HAp in composites was seen in phosphates band shifting. This change indicates that there is an electrostatic interaction between HAp particles and GO by the attraction of phosphate ions with oxygen-containing groups of GO through hydrogen bonding.[31] The minor shiftings of phosphates bands are stated below in Table-3.

Table-2: The Crystal Size of GO/HAp and HAp Calculated by the Debye-Scherrer Equation

Samples	2θ	β	k	λ	θ	β rad	θ rad	Cos θ rad	D (Ā)	D (nm)
HAp	31,7509	0,4745	0,9	1,5406	15,8755	0,0083	0,2771	0,9619	174,0321	17,4032
GO-1/HAp	31,8536	0,4125	0,9	1,5406	15,9267	0,0072	0,2779	0,9616	200,2334	20,0233
GO-2/HAp	31,7132	0,3166	0,9	1,5406	15,8565	0,0055	0,2767	0,9619	260,8444	26,0844
GO-3/HAp	31,7209	0,3239	0,9	1,5406	15,8604	0,0056	0,2768	0,9619	254,9670	25,4967

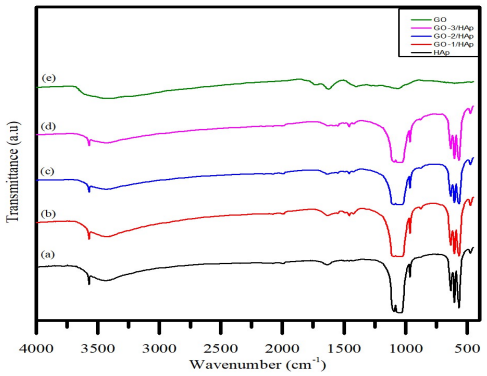

Fig.-3: Absorption Spectrum of GO, GO/HAp, and HAp

Table-3: The Shiftings of Absorbed Bands of Phosphates

Absorbed bands	Wavenumber (cm^1)			
	HAp	GO-1/HAp	GO-2/HAp	GO-3/HAp
Vibration (v1) PO_4^{3-}	1091,92	1092,50	1093,00	1090,91
Vibration (v3) PO_4^{3-}	1041,50	1049,00	1049,50	1047,00
Vibration (v4) PO_4^{3-}	563,02	564,43	564,51	565,33

Morphological Analysis of GO/HAp Composite and HAp

The SEM image of HAp is presented in Fig.-4a. It confirmed that HAp had an agglomerated rod-like structure with most particles in size between 80–100 nm. Next to that, Fig.-4b shows the surface morphology of the GO-2/HAp composite. It depicts that HAp particles were deposited and covered the surface of GO sheets. This is due to during addition of calcium nitrate into the dispersion of GO, followed by the inclusion of phosphates ions into the mixture. The nucleation of apatite happened on the edges and on the lattice lateral of GO sheets, in which role GO acted as the anchor site for the composite to occur.[32] This is also confirmed by FT-IR analysis, where composites resulted from the electrostatic interaction happened between GO layers and HAp. Along with that, the presence of calcium (Ca), phosphate (P), and oxygen (O) composition of HAp was defined by an EDAX spectroscopy, as can be seen in Fig.-4c. Therefore, the Ca/P ratio of HAp was calculated by EDAX measurement to 1.84.

CONCLUSION

The results demonstrated that GO/HAp and HAp were successfully fabricated using scallop shells as calcium sources through the in-situ hydrothermal method. The XRD analysis suggested that HAp has a

hexagonal structure, and also, the GO addition into the hybrid system did not alter the crystal structure of HAp. This was confirmed by FT-IR analysis that the composite resulted from the physical interaction between the matrix and reinforced through a hydrogen bond. Also, from SEM observation, we can see that rod-like particles of HAp were assembled on top and on the edges of the GO surface during the reaction. The ratio Ca/P of the obtained HAp was found to be 1.84, which was confirmed by EDAX analysis.

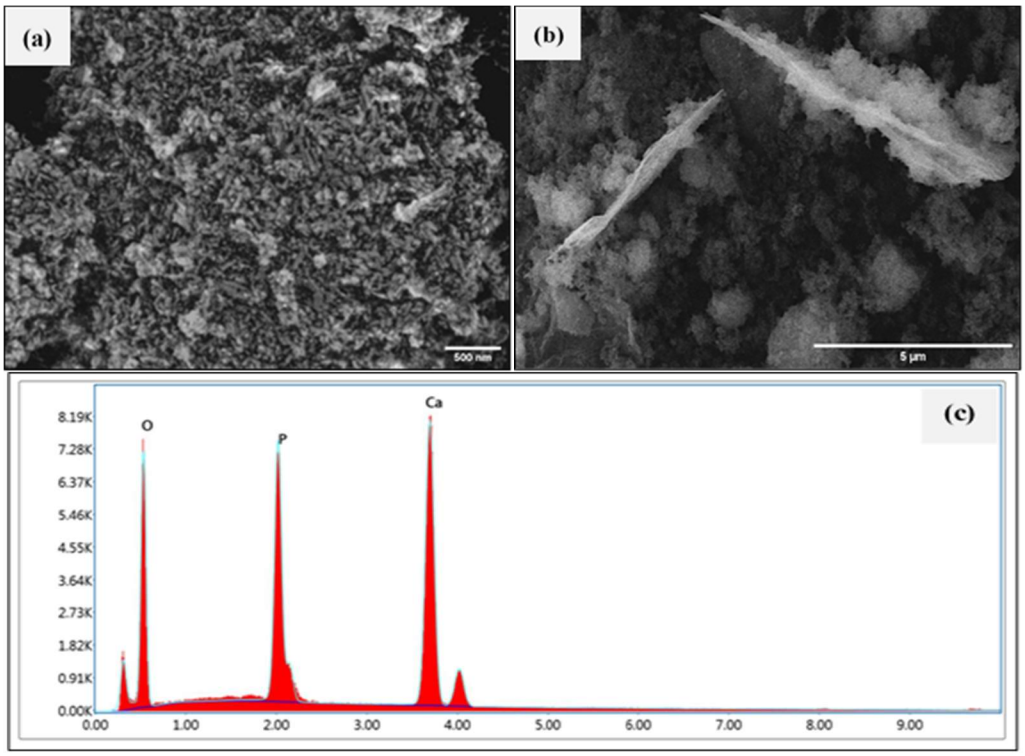

Fig-4: SEM Illustration of (a) HAp, (b) GO-2/HAp, and (c) EDAX Analysis

ACKNOWLEDGMENTS

This research was financially supported by the Ministry of Education, Culture, Research, and Technology of the Republic of Indonesia (Direktorat Jenderal Pendidikan Tinggi, Kementerian Pendidikan dan Kebudayaan Indonesia) through the national competitive grant [Grant number 086/E5/P6.02.00.PT/2022].

CONFLICT OF INTERESTS

The authors declare that there is no conflict of interests.

AUTHOR CONTRIBUTIONS

All the authors contributed significantly to this manuscript, participated in reviewing/editing and approved the final draft for publication. The research profile of the authors can be verified from their ORCID ids, given below:

D. M. Islami https://orcid.org/0000-0001-7014-6521
Wulandari http://orchid.org/0000-0002-7064-9978
N. Jamarun http://orchid.org/0000-0001-8284-145X
Syukri http://orchid.org/0000-0001-5078-0170
V. Sisca http://orchid.org/0000-0001-9325-5990

Open Access: This article is distributed under the terms of the Creative Commons Attribution 4.0 International License (http://creativecommons.org/licenses/by/4.0/), which permits unrestricted use, distribution, and reproduction in any medium, provided you give appropriate credit to the original author(s) and the source, provide a link to the Creative Commons license, and indicate if changes were made.

REFERENCES

1. S. Thomas, B.S.P. Harshita, P. Mishra and S. Talegaonkar, *Current Pharmaceutical Design*, **21(42),** 6165(2015), https://doi.org/10.2174/1381612821666151027153246
2. Charlena, A. Bikharudin, S. T. Wahyudi and Erizal, *Rasayan Journal of Chemistry*, **10(3)**, 766(2017), https://doi.org/10.7324/RJC.2017.1031768
3. D. S. Gomes, A. M. C. Santos, G. A. Neves and R. R. Menezes, *Ceramica*, **65(374),** 282(2019) https://doi.org/10.1590/0366-69132019653742706
4. I. Zia, R. Jolly, S. Mirza, A. Rehman and M. Shakir, *ChemistrySelect*, **7(3)**, e202103234(2022), https://doi.org/10.1002/slct.202103234
5. S. Baradaran, E. Moghaddam, W. J. Basirun, M. Mehrali, M. Sookhakian, M. Hamdi, M. R. N. Moghaddam and Y. Alias, *Carbon,* **69**, 32(2014), https://doi.org/10.1016/j.carbon.2013.11.054
6. S. Klébert, C. Balázsi, K Balázsi, E. Bódis, P. Fazekas, A. M. Keszler, J. Szépvőlgyi and Z. Károly, *Ceram Int*, **41(3)**, 3647(2015), https://doi.org/10.1016/j.ceramint.2014.11.033
7. S. Singh, K. K. Pandey, O. S. Asiq Rahman, S. Haldar, D. Lahiri and A. K. Keshri, *Materials Research Express*, **7(1)**, 015415(2020), https://doi.org/10.1088/2053-1591/ab6c23
8. M. Li, P. Xiong, F. Yan, S. Li, C. Ren, Z. Yin, A. Li, H. Li, X. Ji, Y. Zheng and Y. Cheng, *Bioactive Materials*, **3(1)**, 1(2018), https://doi.org/10.1016/j.bioactmat.2018.01.001
9. G. Bharath, B. S. Latha, E. H. Alsharaeh, P. Prakash and N. Ponpandian, *Analytical Methods*, **9(2)**, 240(2017), https://doi.org/10.1039/c6ay02348g
10. I. Iacoboni, F. Perrozzi, L. Macera, G. Taglieri, L. Ottaviano and G. Fioravanti, *Journal Biomedical Materials Research - Part A*, **107(9)**, 2026(2019), https://doi.org/10.1002/jbm.a.36716
11. S. Basak and G. Packirisamy, *ChemistrySelect*, **6(36)**, 9669(2021), https://doi.org/10.1002/slct.202101975
12. A. R. Noviyanti, D. R. Eddy, Rukiah and Y. Deawati, *Rasayan Journal of Chemistry*, **14(2),** 1006(2021), https://doi.org/10.31788/RJC.2021.1426255
13. Y. Li, C. Liu, H. Zhai, G. Zhu, H. Pan, X. Xu and R. Tang, *RSC Advances*, **4(48)**, 25398(2014), https://doi.org/10.1039/c4ra02821j
14. N. Jamarun, Z. Azharman, S. Arief, T. P. Sari, A. Asril and S. Elfina, *Rasayan Journal of Chemistry*, **8(1)**, 133(2015)
15. N. Jamarun, A. Asril, Zulhadjri, Z. Azharman and T. P. Sari, *Journal of Chemical and Pharmaceutical Research*, **7(6)**, 832(2015)
16. A. X. S. Sebastin and V. Uthirapathy, *ChemistrySelect*, **5(39)**, 12140(2020), https://doi.org/10.1002/slct.202003368
17. G. Karunakaran, E. B. Cho, G. S. Kumar, E. Kolesnikov, G. Janarthanan, M. M. Pillai, S. Rajendran, S. Boobalan, K. G. Sudha, M. P. Rajeshkumaur, *Ceramics International*, **46(18),** 28514(2020), https://doi.org/10.1016/j.ceramint.2020.08.009
18. A. Hart, *Waste Manag Res*, **38(5)**, 514(2020), https://doi.org/10.1177/0734242X19897812
19. Y. Aziz, N. Jamarun, C. D. Alfarisi, A. Mutamima, Komalasari, Nurfatihayati and V. Sisca, *Rasayan Journal of Chemistry,* **15(1),** 96(2022), https://doi.org/10.31788/RJC.2022.1516635
20. N. Jamarun, Yulfitrin and S..Arief, *Jurnal Riset Kimia*, **1(1)**, 20(2015), https://doi.org/10.25077/jrk.v1i1.54
21. S. Muljani, E. A. Saputra and K. Sumada, *Reaktor*, **21(1)**, 27(2021), https://doi.org/10.14710/reaktor.21.1.27-34
22. J. Sun, L. Wang and D. Zhao, *Chinese Journal of Chemical Engineering*, **25(9)**, 1335(2017), https://doi.org/10.1016/j.cjche.2016.12.004
23. N. Jamarun, A. Asril, Z. Zilfa and U. Septiani, *International Journal of Applied Pharmaceutics*, **10(1),** 136(2018), https://doi.org/10.22159/ijap.2018v10i1.23278
24. N. Jamarun, Z. Azharman, Zilfa and U. Septiani, *Oriental Journal of Chemistry*, **32(4)**, 2095(2016), https://doi.org/10.13005/ojc/320437
25. B. Y. Wang, S. Hsu, C. M. Chou, T. I. Wu and V. K. S. Hsiao, *Nanomaterials*, **11(4),** 986(2021), https://doi.org/10.3390/nano11040986

26. X. Mei, X. Meng and F. Wu, *Physica E: Low-Dimensional Systems and Nanostructures*, **68**, 81(2015), https://doi.org/10.1016/j.physe.2014.12.011
27. H. Nosrati, R. S. Mamoory, F. Dabir, D. Q. Svend Le, C. E. Bünger, M. C. Perez and M. A. Rodriguez, *Ceramics International*, **45(2)**, 1761(2019), https://doi.org/10.1016/j.ceramint.2018.10.059
28. A. Michelot, S. Sarda, C. Audin, E. Deydier, E. Manoury, R. Poli and C. Rey, *Journal of Materials Science*, **50(17)**, 5746(2015), https://doi.org/10.1007/s10853-015-9122-x
29. K. Prabakaran, A. Balamurugan and S. Rajeswari, *Bulletin of Materials Science*, **28(2)**, 115(2005), https://doi.org/10.1007/BF02704229
30. P. E. Timchenko, E. V. Timchenko, E. V. Pisareva, M. Y. Vlasov, N. A. Red'kin and O. O. Frolov, *Journal of Physics: Conference Series*, **784**, 012060(2017), https://doi.org/10.1088/1742-6596/784/1/012060
31. M. G. Raucci, D. Giugliano, A. Longo, S. Zeppetelli, G. Carotenuto and L. Ambrosio, *Journal of Tissue Engineering Regenerative Medicine*, **11(8)**, 2204(2017), https://doi.org/10.1002/term.2119
32. Z. Yang, J. Liu, J. Liu, X. Chen, T. Yan and Q. Chen, *Journal of Australian Ceramic Society*, **57(2)**, 625(2021), https://doi.org/10.1007/s41779-021-00568-3

[RJC-8169/2022]